World Journal of Gastroenterology

Submit a Manuscript: http://www.wjgnet.com/esps/
Help Desk: http://www.wjgnet.com/esps/helpdesk.aspx
DOI: 10.3748/wjg.v21.i14.4334

World J Gastroenterol 2015 April 14; 21(14): 4334-4344
ISSN 1007-9327 (print) ISSN 2219-2840 (online)

META-ANALYSIS

Superparamagnetic iron oxide-enhanced magnetic resonance imaging for focal hepatic lesions: Systematic review and meta-analysis

You-Wei Li, Zheng-Guang Chen, Ji-Chen Wang, Zong-Ming Zhang

You-Wei Li, Department of Radiology, Beijing Chuiyangliu Hospital Affiliated to School of Medicine, Tsinghua University, Beijing 100022, China
Zheng-Guang Chen, Department of Radiology, Dongzhimen Hospital Affiliated to Beijing University of Chinese Medicine, Beijing 100700, China
Ji-Chen Wang, Department of Radiology, Nanjing BenQ Hospital, Nanjing 210036, Jiangsu Province, China
Zong-Ming Zhang, Department of General Surgery, Beijing Electric Power Hospital, Capital Medical University, Beijing 100073, China
Author contributions: Zhang ZM designed the study; Li YW, Chen ZG and Wang JC searched and reviewed the literature; Wang JC provided analytic tools and analyzed the data; Li YW and Chen ZG wrote the paper.

Correspondence to: Zong-Ming Zhang, MD, PhD, Professor, Director, Department of General Surgery, Beijing Electric Power Hospital, Capital Medical University, No. 1 Taipingqiaoxili, Fengtai District, Beijing 100073, China. zhangzongming@mail.tsinghua.edu.cn
Telephone: +86-10-63503046
Fax: +86-10-63465865
Received: September 9, 2014
Peer-review started: September 10, 2014
First decision: October 14, 2014
Revised: October 25, 2014
Accepted: November 19, 2014
Article in press: November 19, 2014
Published online: April 14, 2015

Abstract

AIM: To evaluate the performance of superparamagnetic iron oxide (SPIO)-enhanced magnetic resonance imaging (MRI) in the detection and characterization of focal hepatic lesions (FHLs).

METHODS: This meta-analysis compared relevant studies that were identified by searching PubMed, EMBASE, and the Cochrane Library databases for articles published between January 1988 and September 2014 and that met the following criteria: (1) SPIO-enhanced MRI was conducted to identify FHLs and data were sufficient for pooled analysis using Meta-DiSc 1.4; (2) hepatocellular carcinomas (HCCs) were differentiated from other FHLs; (3) well-differentiated HCCs (WD-HCCs) were contradistinguished from dysplastic nodules; and (4) WD-HCCs were compared with moderately and poorly differentiated HCCs (MD- and PD-HCCs, respectively).

RESULTS: The data obtained from 15 eligible studies yielded a sensitivity of 85% and a specificity of 78% for differentiating between HCCs and other FHLs. The sensitivity was unchanged and the specificity was increased to 87% when non-HCC malignancies were excluded. Comparative analyses between WD-HCCs and MD- and PD-HCCs from seven studies showed a sensitivity of 98% and a specificity of 50% for the diagnosis of MD- and PD-HCCs, and the area under the summary receiver operating characteristics (sROC) curve was 0.97. A comparison between WD-HCCs and dysplastic nodules revealed a sensitivity of 50% and a specificity of 92% for the diagnosis of WD-HCCs and the area under the sROC curve was 0.80.

CONCLUSION: SPIO-enhanced MRI is useful in differentiating between HCCs and other FHLs.

Key words: Hepatocellular carcinomas; Magnetic resonance imaging; Meta-analysis; Other lesions; USPIO

Core tip: Relevant studies on the performance of superparamagnetic iron oxide (SPIO)-enhanced magnetic resonance imaging (MRI) in the detection and characterization of focal hepatic lesions were identified by searching PubMed, EMBASE, and the Cochrane Library databases for articles published between January 1988 and September 2014 *via* a systematic review and meta-analysis. The results show that SPIO-enhanced MRI is useful in differentiating between hepatocellular carcinomas (HCCs) and other focal hepatic lesions. Using hyperintensity on SPIO-enhanced T2*-weighted images as the criterion, the sensitivity for diagnosing advanced HCC was 98%. SPIO-enhanced MRI is a valuable tool for the detection and characterization of focal lesions in cirrhotic liver.

Li YW, Chen ZG, Wang JC, Zhang ZM. Superparamagnetic iron oxide-enhanced magnetic resonance imaging for focal hepatic lesions: Systematic review and meta-analysis. *World J Gastroenterol* 2015; 21(14): 4334-4344 Available from: URL: http://www.wjgnet.com/1007-9327/full/v21/i14/4334.htm DOI: http://dx.doi.org/10.3748/wjg.v21.i14.4334

INTRODUCTION

Hepatocellular carcinoma (HCC) is one of the most common cancers, and the third leading cause of cancer-related death worldwide. During the last two decades, progress in multimodality therapy has increased the rate of survival and improved the quality of life for patients with HCC. However, the overall prognosis of HCC is still poor and early diagnosis remains the key to improving prognosis. HCC often arises from the liver with chronic hepatitis B or C virus infection or cirrhosis[1]. Based on the concept of stepwise hepatocarcinogenesis, HCC is considered to develop from a regenerative nodule to a dysplastic nodule (DN), and subsequently to a well-differentiated HCC (WD-HCC) and an advanced tumor [moderately differentiated (MD) and poorly differentiated (PD) HCCs]. WD-HCC has a relatively low malignant potential and rarely invades vessels or metastasizes to other sites. Patients with WD-HCC usually have a better survival rate than those with MD- or PD-HCC[1].

In clinical practice, it is critical to differentiate WD-HCC from advanced HCC and from other focal hepatic lesions (FHLs). Various imaging modalities have been used in the detection and characterization of HCCs, including ultrasonography (US), computed tomography (CT), magnetic resonance imaging (MRI), and positron emission tomography. MRI, especially dynamic contrast-enhanced MRI, provides better tissue contrast than US and CT, and is considered to be one of the most sensitive modalities for the diagnosis of HCC[2,3]. Currently, two types of MRI contrast agents have been used in liver MRI, extracellular fluid contrast agents such as gadolinium (Gd) chelates and liver-specific contrast agents such as superparamagnetic iron oxide (SPIO). Gd-enhanced MRI is based on the blood flow of lesions, while SPIO-enhanced MRI is largely dependent on the number and function of Kupffer cells in lesions. SPIO particles are taken up by Kupffer cells and predominantly shorten the T2 of hepatic parenchyma. Normal hepatic parenchyma and some FHLs contain Kupffer cells and therefore exhibit decreased signal intensity, whereas hepatic lesions without Kupffer cells show less or no change in signal intensity. In the case of lesions with Kupffer cells, the lesion-parenchyma contrast is enhanced, and thus the lesions are conspicuous on T2- and T2*-weighted MRI.

In recent years, the value of SPIO in the detection and characterization of FHLs has been emphasized and studies have demonstrated its usefulness[4-6]. In particular, SPIO-enhanced MRI is currently considered to be the only imaging modality that is capable of distinguishing HCC from DN, although it is limited when both HCC and DN contain a similar number of Kupffer cells[7-9]. The aim of this study was to determine the diagnostic performance of SPIO-enhanced MRI in differentiating between HCC and other FHLs *via* a systematic review and meta-analysis of the studies published on this topic.

MATERIALS AND METHODS

Study selection

PubMed, EMBASE, and the Cochrane Library databases were searched for articles published between January 1988 and September 2014. Eligible studies included those in which SPIO-enhanced MRI was conducted in patients with HCC or other hepatic lesions. The search strategy was: magnetic resonance imaging, MRI, or MR imaging and carcinoma, hepatocellular, liver neoplasms, liver lesion, HCC, or hepatic lesions and ferumoxtran-10, SPIO or USPIO. We identified additional articles by crosschecking related citations in the retrieved studies.

The inclusion criteria used in this meta-analysis were as follows: (1) MRI was conducted at a field strength of at least 0.5 T; (2) the diagnostic criteria for HCC and other malignant or benign lesions such as DN, focal nodular hyperplasia, and hemangioma, were clearly documented; (3) data were obtained with T2- or T2*-weighted MRI after intravenous injection of SPIO contrast agents; and (4) data were on a per-lesion basis and sufficient to construct a 2 × 2 contingency table so that the cells in the table could be labeled as true-positive (TP), false-positive (FP), true-negative (TN), or false-negative (FN). Studies were included when all criteria were met.

Four steps were used to select the articles for inclusion in this study. First, one reviewer screened the titles of all research articles identified from the database. Articles were selected when the studies met some of the inclusion criteria. Second, two reviewers screened the abstract of the selected articles

independently and the articles were further assessed if the information was sufficient. Third, the eligible full articles were obtained through online sources, library visits, and interlibrary loan requests. The full papers were then reviewed independently by two reviewers to decide whether the reported studies should be included. Disagreement between the two reviewers was resolved by consensus or by a third reviewer. The references listed in the selected articles were also searched to identify further relevant articles. Finally, the quality of all included articles was evaluated based on the quality assessment of diagnostic accuracy studies (QUADAS)[10].

Data extraction

To meta-analyze the diagnostic accuracy in different hepatic lesions and to calculate the number of TP, FP, FN, and TN results in each study, data were extracted using the following criteria: the lesions with iso- or hypointensity on SPIO-enhanced MR images were considered negative. The lesions with hyperintensity with a focal, high signal intensity were classified as positive. If there were two sets of data obtained by T2- and T2*-weighted imaging in the same study, the data obtained by T2*-weighted imaging were extracted as susceptibility is maximized on this sequence. Data extracted from studies also included some general information: publications (first author, country, language, and date of publication), patients and lesions (number and mean age of patients, and number, type and mean size of lesions), MRI (magnetic field strength, sequence, contrast agent, and dosage), and MR image evaluation (criteria used to confirm the lesions, and whether the interpreters of the MR images were blinded to clinical information and/or the reference-standard examination results).

To evaluate the diagnostic performance of SPIO-enhanced MRI in FHLs, the extracted data were subgrouped according to the lesion's characteristics and a comparison was made between: (1) HCC and all other lesions (benign and non-HCC malignant lesions); (2) HCC and benign lesions; (3) WD-HCC and DN; and (4) WD-HCC and advanced HCC (MD- and PD-HCC).

Pooled analysis

The software Meta-DiSc version 1.4 (http://www.hrc.es/investigation/metadisc-en.htm) was used for the meta-analysis. The sensitivity and specificity were calculated using the formulas of TP/(TP + FN) and TN/(TN + FP), respectively. The diagnostic odds ratio (DOR) was calculated using the formula of (TP*TN)/(FP*FN). If the DOR could not be calculated when one of the cells in the 2 × 2 table was zero, 0.5 was added to all cells in that study.

First, a forest plot was used to assess the accuracy of the sensitivity and specificity in each study and to evaluate the heterogeneity across studies. One of the primary reasons for the heterogeneity among studies is the threshold effect. This issue may arise when different cut-off values or thresholds are used to define a positive or a negative test result. Therefore, we considered that the threshold effect existed when the forest plots showed increasing sensitivities along with decreasing specificities, or *vice versa*. In this case, Spearman rank correlation was used as a further test for the threshold effect and an inverse correlation between sensitivity and specificity indicated the presence of the threshold effect. Considering that some other factors might also result in heterogeneity among studies, we also assessed the heterogeneity using the Cochran *Q*, χ^2 and I^2 tests. When the Cochran *Q* test was significant or the I^2 > 50%, heterogeneity was considered to exist.

Second, we calculated the pooled sensitivity and specificity. If heterogeneity due to the threshold effect was present, the accuracy data were pooled by fitting the summary receiver operating characteristics (sROC) curve, and the area under the curve and *Q** (defined by the point where sensitivity equaled specificity) were calculated. In cases where heterogeneity was due to sources other than the threshold effect, the random effects model (DerSimonian-Laird method) was used instead of the fixed effects model (Mantel-Haenszel method) for calculation of pooled sensitivity and specificity with a 95%CI. The asymmetric sROC curve was reconstructed with Moses' model regression.

Third, meta-regression analysis was performed by extending the Moses-Shapiro-Littenberg method to explore the sources of heterogeneity among studies. The covariates evaluated in this study included the number and mean size of lesions, the mean age of patients, the magnetic field strength and imaging sequence, the contrast agent and dosage, the criteria used to confirm the characteristics of lesions, and whether the interpreter of the MR images was blinded to clinical information and/or the reference-standard examination results. Because the number of studies was small, we tested one covariate at a time. A $P < 0.05$ was considered significant.

RESULTS

Study selection and data extraction

A total of 365 relevant articles were initially identified, of which 236 studies were excluded after reviewing the titles. Abstract review of the remaining 129 studies by two reviewers excluded an additional 105 studies. Twelve articles were added after checking the related citations and by screening the reference list of the included articles. On review of the full-texts of the 36 articles, 15 eligible studies were included and data were extracted (Table 1) for meta-analysis (Figure 1). Almost perfect agreement (κ = 0.95) was achieved between the two reviewers during selection of the articles.

The total number of hepatic lesions in the 15 studies was 958, ranging from 10 to 216. The majority of lesions were confirmed pathologically and a few

Table 1 Characteristics of 15 studies included in the meta-analysis

Ref.	Year	Country	Subject					MRI				Result	
			Patients (*n*)	Age (yr)	Lesions (*n*)	Lesion type	Size (cm)	Type	Sequence	Contrast agent	Dose	Iso-/hypo	Hyper-
Harisinghani *et al*[12]	1997	United States	35	46	15	Hemangioma	NC	1.5T	T2WI	Code-7227	1.1 mg Fe/kg	13	2
					17	Metastases	NC					0	17
					6	HCC	NC					2	4
Imai *et al*[19]	2000	Japan	27	62	6	DN	1.6	1.5T	T2*WI	Ferumoxide	10 μmol/kg	6	0
					13	WD-HCC	1.6					11	2
					10	MD-HCC	1.6					0	10
					8	PD-HCC	1.6					0	8
Lim *et al*[15]	2001	South Korea	68	51	10	WD-HCC	2.1	1.5T	T2*WI	Ferumoxide	15 μmol/kg	6	4
					69	MDPD-HCC	5.3					0	69
					19	DN	0.8					19	0
Zheng *et al*[11]	2002	China	43	51	22	HCC	< 3	1.5T	T2WI	Feridex	0.05 mL/kg	0	22
					7	Other malignancy	< 3					0	7
					4	Cirrhotic nodules	< 3					4	0
					5	Hemangioma						0	5
					5	FNH						0	5
					4	Others						0	4
Zhang *et al*[20]	2003	China	30	50	30	HCCs	NC	0.5T	T2WI	Feridex	0.56 mL/kg	0	30
					6	Regenerative nodules						6	0
Suzuki *et al*[21]	2004	Japan	45	66	41	HCCs	2.26	1.5T	T2*WI	Ferumoxide	0.05 mL/kg	7	34
					11	Benign						10	1
Kato *et al*[22]	2004	Japan	43	66	17	WD-HCC	3.00	1.5T	T2*WI	Ferumoxide	10 mmol/kg	4	13
					28	MD-HCC	3.00					1	27
					6	PD-HCC	3.20					0	6
Inoue *et al*[24]	2005	Japan	49	67	20	WD-HCC	2.70	1.5T	T2*WI	Ferumoxide	0.016 mL/kg	4	16
					20	MDPD-HCC						0	20
					9	DNs						8	1
Kobayashi *et al*[9]	2007	Japan	10	45	6	DNs	NC	1.5T	T2WI	Ferucarbotran	NC	6	0
					4	HCC						0	4
Park *et al*[18]	2009	South Korea	114	55	37	WD-HCC	2.38	3.0T	T2*WI	Ferucarbotran	8 mmol/kg	20	17
					156	MDPD-HCC	4.10					6	149
					23	DNs	1.28					22	1
Macarini *et al*[7]	2009	Italy	22	53	14	HCC	1.70	1.5T	T2*WI	Ferumoxide	NC	0	14
					3	WD-HCC							
					11	MDPD-HCC							
					4	DN with HCC	2.10					0	4
					39	DNs	0.80					39	0
					2	Cystadenoma	1.20					2	0
Yoon *et al*[16]	2009	South Korea	28	51	33	DNs	1.31	3.0T	T2*WI	Ferucarbotran	1.4 mL, ⩾ 60 kg	25	8
					32	WD-HCC	1.79				0.9 mL, < 60 kg	13	19
Yoo *et al*[8]	2009	South Korea	108	56	124	HCCs	3.00	3.0T	T2*WI	Ferucarbotran	1.4 mL, ⩾ 60 kg	16	108
					28	DNs					0.9 mL, < 60 kg	25	3
Okada *et al*[23]	2010	Japan	36	69	22	WD-HCC	1.40	1.5T	T2*WI	Ferucarbotran	0.45 mg Fe/kg	15	7
					15	MDPD-HCC	2.40					0	15
					4	DNs	1.60					4	0
Chou *et al*[25]	2011	Taiwan	12	56	11	HCC	2.30	1.5T	T2*WI	Ferucarbotran	1.4 mL, > 50 kg	3	8
					6	Benign	1.60					6	0

DN: Nodular dysplasia; FNH: Focal nodular hyperplasia; HCC: Hepatocellular carcinoma; hyper: Hyperintensity; iso-/hypo: Isointensity/hypointensity; MD: Moderately-differentiated, NC: Not clear; PD: Poorly-differentiated; WD: Well-differentiated; MRI: Magnetic resonance imaging.

were diagnosed on the basis of clinical findings, biochemical tests, and clinical follow-up (⩾ 6 mo). The pathologic specimens in all studies were obtained by needle biopsy, hepatic resection, or transplantation, except in two studies[11,12], in which the acquirement of specimens was not clearly stated. HCC was graded pathologically as WD-HCC, MD-HCC, and PD-HCC, according to the classification criteria of primary hepatic cancer by the Liver Cancer Study Group of Japan[13]. DN was defined using the criteria of the International Working Party on the Terminology of Nodular Hepatocellular Lesions[14].

We assessed the quality of the 15 studies using the 13-item QUADAS tool. All studies had an overall score of 10 or more, except one study that had a score of 6 (Table 2)[11]. Four of the 13 items were scored as "1" in all studies, including item 2 (clearly describing selection criteria), item 7 (execution of

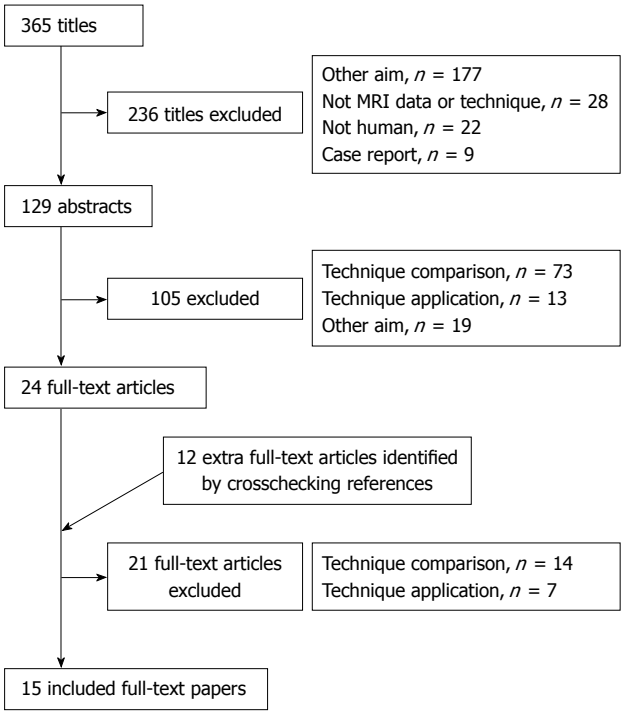

Figure 1 Flow chart of process used to select eligible articles.

the index test described in sufficient detail to permit its replication), item 12 (reporting of uninterpretable results), and item 13 (explanation of withdrawals from the study). Four of the 15 items were scored as "1" in 13/15 to 14/15 studies, including item 1 (the spectrum of tested patients representing the patients in whom the test will be used in practice), item 3 (the reference standard likely to correctly classify the target condition), item 5 (the whole sample receiving verification using a reference standard of diagnosis), and item 6 (patients receiving the same reference standard regardless of the index test result). Some items were poorly reported, which yielded various levels of bias. Item 9, related to information on clinical data during interpretation of test results, might affect the estimates of test performance as it was not reported clearly in any of the included studies. The period between the reference standard and index test, which might cause disease progression bias, was reported only in three studies. Nearly half of the studies insufficiently described the reference standard test, which may have had an impact on the test performance. Two other items that were reported in less than 50% of the included studies and might be related to review bias were the index test results interpreted without knowledge of the results of the reference standard (40%) and the reference standard results interpreted without knowledge of the results of the index test (33%).

Pooled analysis

The Spearman rank correlation coefficient used to test accuracy in all studies was -0.266 (P = 0.358) (Table 3), indicating no threshold effect. A comparison between HCC and all other liver lesions from 14 eligible studies showed that the sensitivity for diagnosing HCC was 85% (95%CI: 0.82-0.88) and the specificity was 78% (95%CI: 0.73-0.83). There was substantial heterogeneity across these studies for sensitivity (I^2 = 80.9) and specificity (I^2 = 89.0)

Table 2 Quality assessment of diagnostic accuracy studies scores[1] for each included study

Ref.	QUADAS items												
	1	2	3	4	5	6	7	8	9	10	11	12	13
Zheng *et al*[11]	0	1	0	0.5	0	0	1	0	0.5	0.5	0.5	1	1
Imai *et al*[19]	1	1	1	0.5	1	1	1	0	1	0.5	0.5	1	1
Lim *et al*[15]	1	1	1	0.5	1	1	1	1	0.5	1	0.5	1	1
Zhang *et al*[20]	1	1	1	0.5	1	1	1	0	0.5	1	0.5	1	1
Inoue *et al*[24]	1	1	1	0.5	1	1	1	1	0.5	1	0.5	1	1
Park *et al*[18]	1	1	1	0.5	1	1	1	1	0	0.5	0.5	1	1
Macarini *et al*[7]	1	1	1	1	1	1	1	0	1	0.5	0.5	1	1
Yoon *et al*[16]	1	1	1	0.5	1	1	1	1	1	1	0.5	1	1
Harisinghani *et al*[12]	1	1	1	0.5	0	1	1	1	1	0.5	0.5	1	1
Yoo *et al*[8]	1	1	1	0.5	1	1	1	1	0	0.5	0.5	1	1
Suzuki *et al*[21]	1	1	1	0.5	1	1	1	0	0.5	0.5	0.5	1	1
Kobayashi *et al*[9]	1	1	1	0.5	1	1	1	0	1	0.5	0.5	1	1
Kato *et al*[22]	1	1	1	1	1	1	1	1	1	0	0.5	1	1
Okada *et al*[23]	1	1	1	0.5	1	1	1	0.5	0.5	1	1	1	1
Chou *et al*[25]	1	1	1	1	1	1	1	0	0.5	0.5	0.5	1	1

[1]1 = yes; 0 = no; 0.5 = unclear. Quality assessment of diagnostic accuracy studies (QUADAS) items: (1) Was the spectrum of a patient representative of the patients who will receive the test in practice? (2) Were the selection criteria clearly described? (3) Is the reference standard likely to correctly classify the target condition? (4) Is the time period between the index test and reference standard short enough to ensure that the target condition did not change between the two tests? (5) Did the whole sample or a random selection of the sample receive verification using a reference standard of diagnosis? (6) Did patients receive the same reference standard regardless of the index test result? (7) Was the execution of the index test described in sufficient detail to permit replication of the test? (8) Was the execution of the reference standard test described in sufficient detail to permit its replication? (9) Were the index test results interpreted without knowledge of the results of the reference standard? (10) Were the reference standard results interpreted without knowledge of the results of the index test? (11) Were the same clinical data available when the test results were interpreted as would be available when the test is used in clinical practice? (12) Were uninterpretable or intermediate test results reported? (13) Were withdrawals from the study explained?

Table 3 Assessment of the threshold effect in all accuracy studies

Weighted regression (inverse variance)				
Variable	**Coefficient**	**SE**	***t***	***P* value**
a	3.643	0.548	6.652	0.0000
b(1)	-0.239	0.314	0.760	0.4617

τ^2 = 2.3703 (convergence is achieved after five iterations); Restricted Maximum Likelihood estimation (REML). n = 14; Filter OFF; Add 0.5 to all cells of the studies with zero. Spearman correlation coefficient: -0.266, P = 0.358; Logit (true positive rate) *vs* Logit (false positive rate); Moses' model (D = a + bS).

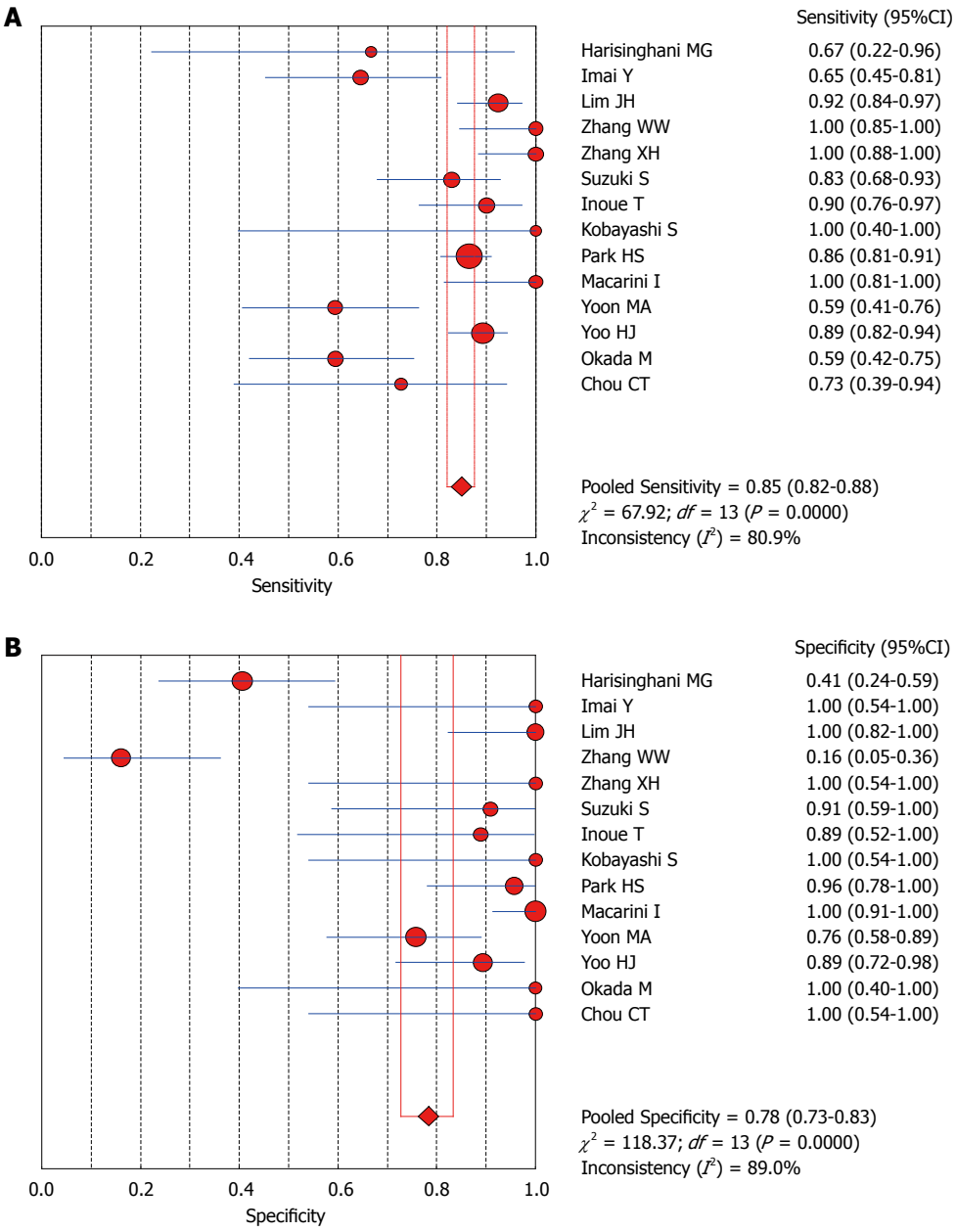

Figure 2 Forest plots for comparing hepatocellular carcinomas with all other liver lesions. A: Sensitivity; B: Specificity of 14 studies.

(Figure 2). The sensitivity was essentially unchanged when comparing HCC with benign liver lesions, but the specificity increased to 87% (95%CI: 0.82-0.91), with substantial heterogeneity across these studies for sensitivity (I^2 = 80.9) and specificity (I^2 = 81.2) (Figure 3). Seven eligible studies were used for a comparative analysis between advanced HCC (MD-/PD-HCC) and WD-HCC, and the sensitivity and specificity for diagnosing advanced HCCs were 0.98 (95%CI: 0.95-0.99) and 0.50 (95%CI: 0.41-0.60), respectively. The heterogeneity across these studies was less for sensitivity (I^2 = 30.9) and slightly larger for specificity (I^2 = 78.4) (Figure 4). The area under the sROC curve for the seven studies used for comparing advanced HCC with WD-HCC was 0.97, and the Q^* was 0.92 (Figure 5A). A comparison between WD-HCC and DN was performed with the data extracted from seven eligible studies, and the pooled sensitivity and specificity for diagnosing WD-HCC were 0.50 (95%CI: 0.41-0.58) and 0.92 (95%CI: 0.87-0.96), respectively, with substantial heterogeneity across these studies for sensitivity (I^2 = 74.4) and specificity (I^2 = 69.9) (Figure 6). The area under the sROC curve was 0.80, and the Q^* was 0.74 (Figure 5B). All calculations for the pooled sensitivity and specificity in the present analysis were based on the random effects model due to notable heterogeneity across the studies.

To explore the possible sources of heterogeneity, we performed meta-regression analysis using the extended Moses-Shapiro-Littenberg method. The results showed that none of the covariates described in Materials and Methods significantly contributed to the

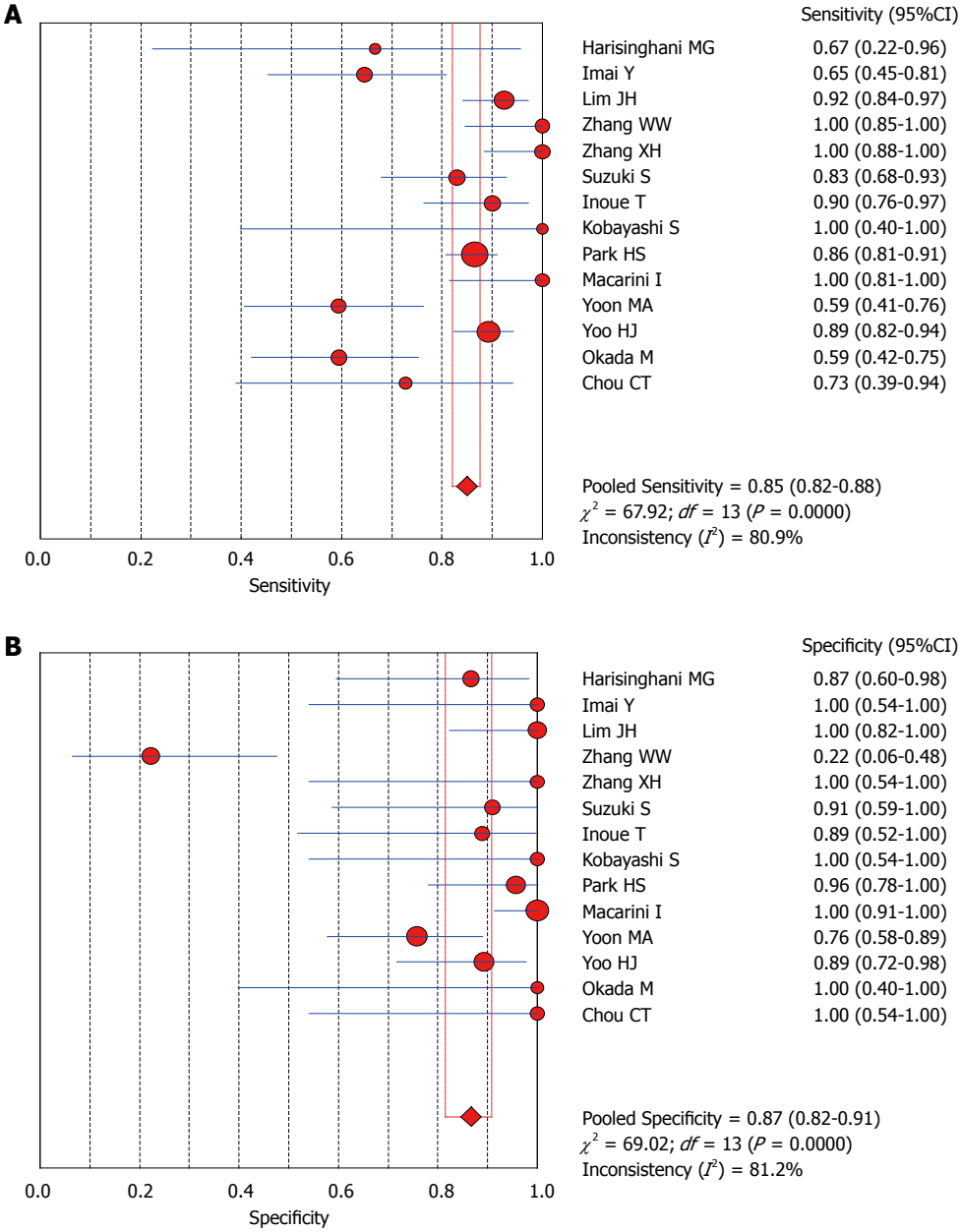

Figure 3 Forest plots for comparing hepatocellular carcinomas with benign liver lesions. A: Sensitivity; B: Specificity of 14 studies.

heterogeneity among the studies.

DISCUSSION

SPIO is a reticuloendothelial cell-specific contrast agent, which is used for the detection and characterization of focal liver lesions, largely based on the number and function of Kupffer cells. SPIO particles are taken up by Kupffer cells and predominantly shorten the T2 of the hepatic parenchyma. Healthy hepatic parenchyma and some focal liver lesions contain Kupffer cells and exhibit decreased signal intensity on SPIO-enhanced MRI, while lesions without Kupffer cells do not show this decrease. The signal intensity difference between lesions and liver parenchyma forms the basis of the detection and characterization of various lesions with SPIO-enhanced MRI. In clinical practice, the signal intensity of a lesion on SPIO-enhanced MR images can be lower (hypointensity) or higher (hyperintensity) than or similar to (isointensity) that of surrounding parenchyma. Because carcinoma lesions often show hyperintensity, we used hyperintensity as a criterion of malignancy to investigate the diagnostic accuracy of SPIO-enhanced MRI in the detection and characterization of focal liver lesions in this systematic review and meta-analysis.

Comparison between HCCs and other hepatic lesions

HCCs usually have different numbers of Kupffer cells, which are highly dependent on their degree of differentiation, whereas other malignant tumors such as metastases and cholangiocarcinoma generally do

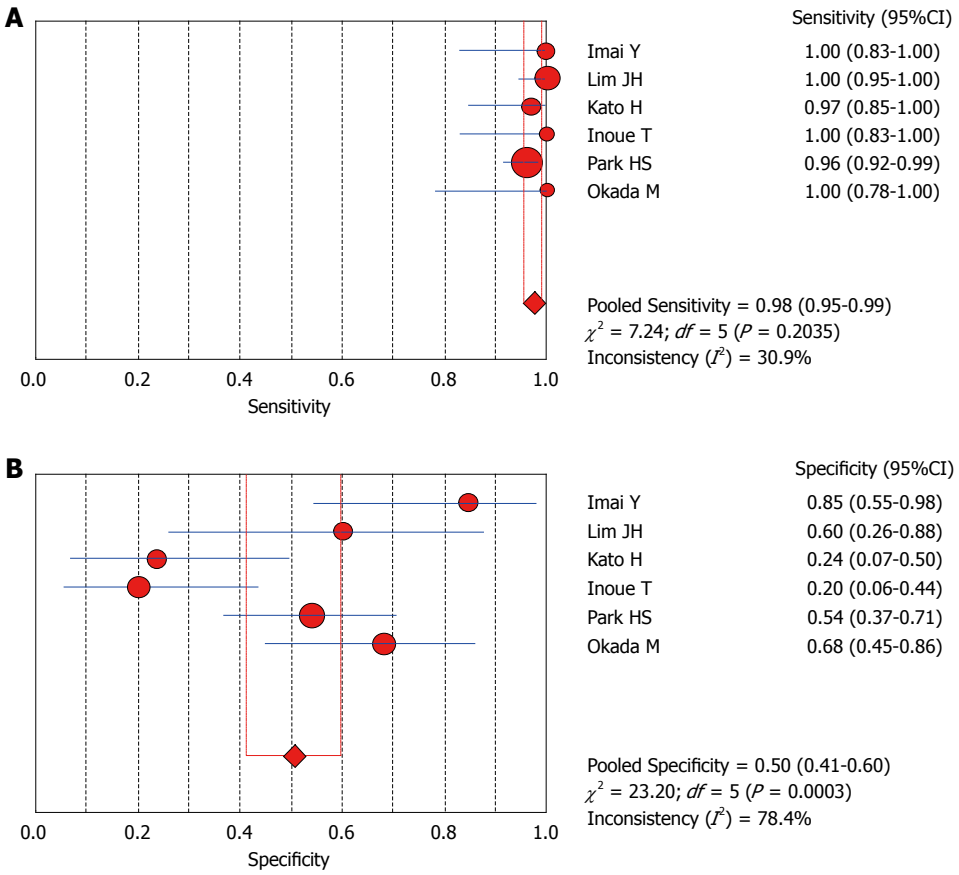

Figure 4 Forest plots for comparing advanced hepatocellular carcinomas with well-differentiated hepatocellular carcinomas. A: Sensitivity; B: Specificity of seven studies.

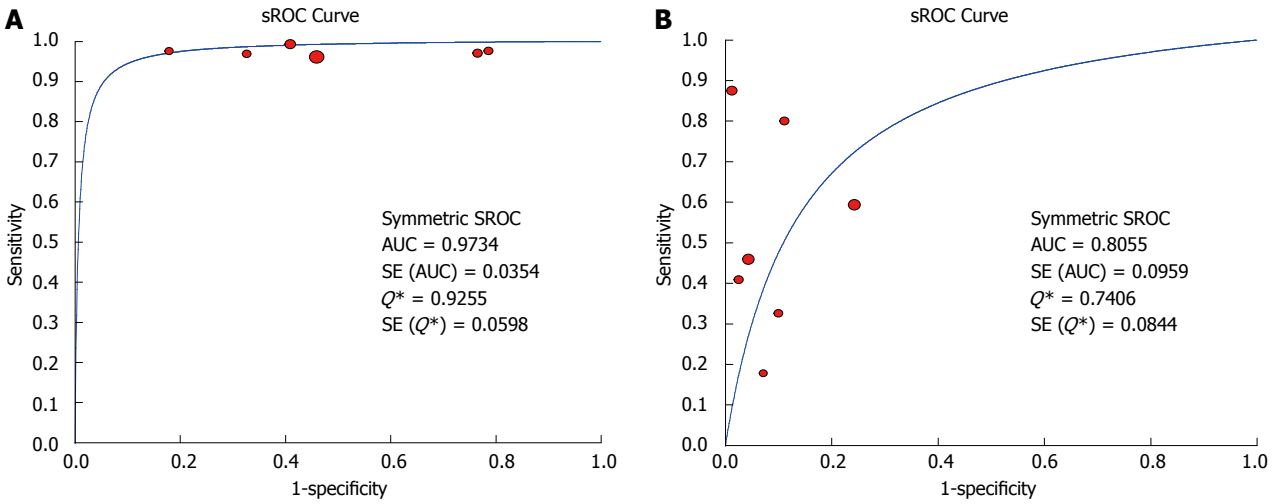

Figure 5 Summary receiver operating characteristics curves. Sensitivity and specificity are plotted for studies comparing advanced hepatocellular carcinomas (HCCs) with well-differentiated HCCs (A) and well-differentiated HCCs with dysplastic nodules (B). AUC: Area under the curve; sROC: Summary receiver operating characteristics.

not have Kupffer cells and exhibit hyperintensity on SPIO-enhanced images. In contrast, most benign lesions including hepatic adenoma, focal nodular hyperplasia, and cirrhotic regenerative nodules, often possess identical or more Kupffer cells than the surrounding parenchyma and thus demonstrate iso- or hypointensity on SPIO-enhanced images[7,15]. As a result, investigators have recently emphasized the value of SPIO-enhanced MRI in the detection and characterization of FHLs[7,8,16].

A comparison between HCCs and all other liver lesions revealed a diagnostic sensitivity of 86%

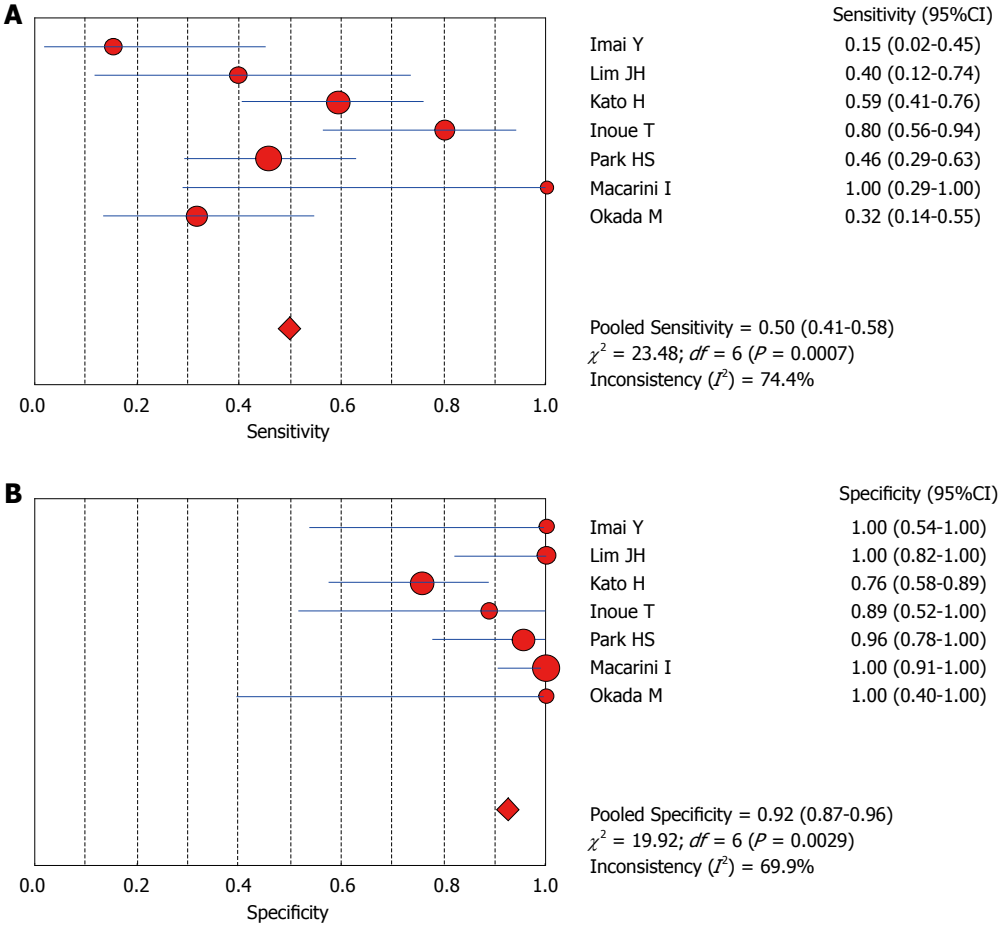

Figure 6 Forest plots for comparing well-differentiated hepatocellular carcinomas with dysplastic nodules. A: Sensitivity; B: Specificity of seven studies.

and a specificity of 76%. When non-HCC malignant lesions were excluded, the estimated sensitivity was essentially unchanged, but the specificity increased to 86%. Although notable heterogeneity existed among the studies, these results support the conclusion that SPIO-enhanced MRI is a valuable tool for the detection and characterization of focal lesions in cirrhotic liver.

Comparison between HCCs and DNs

HCCs develop in a multistep manner from regenerative nodules to DNs that are then transformed into WD-HCCs and advanced HCCs. The malignant transformation takes about 4-6 mo[17]. Precise differentiation of HCCs from DNs is critical for patient outcome. However, differentiation between DNs and HCCs in cirrhotic liver is often difficult because of marked architectural distortion of the parenchyma due to fibrosis, steatosis, necrosis, and regeneration[18].

Nodular hyperplasia and DNs possess identical or slightly more Kupffer cells than the surrounding normal parenchyma[7]. It has been reported that HCCs, especially WD-HCCs, also contain Kupffer cells. Some studies have shown that although there is no significant difference in Kupffer cell number between WD-HCCs and DNs, Kupffer cells are significantly reduced in MD- and PD-HCCs[18,19]. Thus, investigators concluded that SPIO-enhanced MRI can be used to differentiate WD-HCCs from advanced HCCs, but it is difficult to differentiate between WD-HCCs and DNs. Sometimes small WD-HCCs cannot be detected with SPIO-enhanced MRI due to their identical signal intensity to hepatic parenchyma[17].

Our analysis of seven eligible studies showed that the pooled sensitivity for differentiating advanced HCCs (MD/PD-HCCs) from WD-HCCs was 98% with low heterogeneity across these studies. Moreover, the frequency of hyperintensity on SPIO-enhanced MR images was very high in advanced HCCs, though the specificity was low (50%). A comparison between WD-HCCs and DN revealed that the pooled sensitivity and specificity for diagnosing WD-HCCs were 50% and 92%, respectively. These results indicate that both DNs and WD-HCCs may exhibit iso- or hypointensity on SPIO-enhanced MR images, but hyperintensity suggests a high probability of WD-HCCs.

Although the reasons for the heterogeneity among studies were not clear, we noticed an issue in all retrieved studies, *i.e.*, nearly half of the included studies did not report the causes and severity of cirrhosis[11,12,15,20-22]. The causes of liver cirrhosis, such as viral hepatitis B or C, alcoholic liver disease, or an unknown cause, were clearly documented in

other studies[7-9,16,18,19,23-25]. Only five studies reported the severity of cirrhosis based on the Child-Pugh classification[7,8,15,16,23]. Furthermore, none of the studies documented liver function. The functional status of Kupffer cells is more closely correlated with the signal intensity on MRI than the parenchymal pathology and degree of fibrosis[22]. Some investigators have denoted the mismatch between the signal-noise ratio and the number of Kupffer cells, and they consider that the mismatch is mainly due to decreased Kupffer cell function[15]. Therefore, decreased liver and Kupffer cell function may affect the SPIO-enhancement effect on liver parenchyma and lesions in MRI, and thus affect the detection and characterization of focal liver lesions. This may be partially responsible for the heterogeneity observed.

The present study has several limitations. First, potential publication bias may have arisen as some publications might not have been retrieved. In addition, there was notable heterogeneity between the studies. Neither the threshold effect nor the evaluated covariates were the sources and further studies are necessary to identify other parameters that may affect the detection and characterization of focal liver lesions with SPIO-enhanced MRI. Second, there was a considerable lack of reporting on the diagnostic study quality items, particularly QUADAS items 11, 9, 10, and 4. This may have resulted in review bias and disease progression bias. The third limitation in this study was the mandatory correction for zero entries by adding 0.5 to each cell of the study. This may have had an effect on the studies with small sample sizes.

In conclusion, the results of this meta-analysis suggest that SPIO-enhanced MRI is useful for differentiating between HCC and other FHLs as well as between DN and advanced HCC in cirrhotic livers. Using hyperintensity on SPIO-enhanced T2*-weighted images as the criterion, the sensitivity for diagnosing advanced HCC was 98%. SPIO-enhanced MRI is a valuable tool for the detection and characterization of focal lesions in cirrhotic liver.

COMMENTS

Background

Hepatocellular carcinoma (HCC) is the fifth most common malignant tumor worldwide, with 50% of cases occurring in China. The results of treatment are unsatisfactory, as HCC cannot be diagnosed early. Superparamagnetic iron oxide (SPIO) is a reticuloendothelial cell-specific contrast agent, which is widely used for the detection and characterization of focal liver lesions. Although the value of SPIO in the detection and characterization of focal hepatic lesions has been emphasized, some investigators have reported discordant results. Thus, the performance of SPIO-enhanced MRI in focal hepatic lesions still requires further research.

Research frontiers

Meta-analysis is a quantitative, formal, epidemiologic study design used to systematically assess previous research studies to derive conclusions regarding these studies. Outcomes of a meta-analysis may include a more precise estimate of the effect of treatment or risk factor for disease, or other outcomes, than any individual study contributing to the pooled analysis. It can be used to explain discordant findings regarding the value of SPIO in the detection and characterization of focal hepatic lesions, observed with different patient populations.

Innovations and breakthroughs

This meta-analysis included 15 eligible studies to evaluate the diagnostic performance of SPIO-enhanced MRI in focal hepatic lesions. Using hyperintensity on SPIO-enhanced T2*-weighted images as the criterion, the sensitivity for diagnosing advanced HCC was 98%. SPIO-enhanced MRI is a valuable tool for the detection and characterization of focal lesions in cirrhotic liver.

Applications

SPIO-enhanced MRI can be used for differentiating between HCC and other focal hepatic lesions as well as between DN and advanced HCC in cirrhotic livers.

Peer-review

This article evaluated the performance of SPIO-enhanced MRI in detection and characterization of focal hepatic lesions *via* systemic review and meta-analysis. The data showed that SPIO-enhanced MRI was useful for differential diagnosis between HCCs and other focal hepatic lesions. The study was well designed and the methods were accurately applied.

REFERENCES

1 **Lau WY**, Lai EC. Hepatocellular carcinoma: current management and recent advances. *Hepatobiliary Pancreat Dis Int* 2008; **7**: 237-257 [PMID: 18522878]

2 **Kim MJ**, Choi JY, Chung YE, Choi SY. Magnetic resonance imaging of hepatocellular carcinoma using contrast media. *Oncology* 2008; **75** Suppl 1: 72-82 [PMID: 19092275 DOI: 10.1159/000173427]

3 **Goshima S**, Kanematsu M, Kondo H, Shiratori Y, Onozuka M, Moriyama N, Bae KT. Optimal acquisition delay for dynamic contrast-enhanced MRI of hypervascular hepatocellular carcinoma. *AJR Am J Roentgenol* 2009; **192**: 686-692 [PMID: 19234264 DOI: 10.2214/AJR.08.1255]

4 **Teerasamit W**, Saiviroonporn P, Pongpaibul A, Korpraphong P. Benefit of double contrast MRI in diagnosis of hepatocellular carcinoma in patients with chronic liver diseases. *J Med Assoc Thai* 2014; **97**: 540-547 [PMID: 25065095]

5 **Maurea S**, Mainenti PP, Tambasco A, Imbriaco M, Mollica C, Laccetti E, Camera L, Liuzzi R, Salvatore M. Diagnostic accuracy of MR imaging to identify and characterize focal liver lesions: comparison between gadolinium and superparamagnetic iron oxide contrast media. *Quant Imaging Med Surg* 2014; **4**: 181-189 [PMID: 24914419 DOI: 10.3978/j.issn.2223-4292.2014.01.02]

6 **Muhi A**, Ichikawa T, Motosugi U, Sou H, Nakajima H, Sano K, Sano M, Kato S, Kitamura T, Fatima Z, Fukushima K, Iino H, Mori Y, Fujii H, Araki T. Diagnosis of colorectal hepatic metastases: comparison of contrast-enhanced CT, contrast-enhanced US, superparamagnetic iron oxide-enhanced MRI, and gadoxetic acid-enhanced MRI. *J Magn Reson Imaging* 2011; **34**: 326-335 [PMID: 21780227 DOI: 10.1002/jmri.22613]

7 **Macarini L**, Milillo P, Casavilla A, Scalzo G, Stoppino L, Vinci R, Moretti G, Ettorre G. MR characterization of dysplastic nodules and hepatocarcinoma in the cirrhotic liver with hepatospecific superparamagnetic contrast agents: pathological correlation in explanted livers. *Radiol Med* 2009; **114**: 1267-1282 [DOI: 10.1007/s11547-009-0464-9]

8 **Yoo HJ**, Lee JM, Lee JY, Kim SH, Kim SJ, Han JK, Choi BI. Additional value of SPIO-enhanced MR imaging for the noninvasive imaging diagnosis of hepatocellular carcinoma in cirrhotic liver. *Invest Radiol* 2009; **44**: 800-807 [PMID: 19838119 DOI: 10.1097/RLI.0b013e3181bc271d]

9 **Kobayashi S**, Matsui O, Kamura T, Yamamoto S, Yoneda N, Gabata T, Terayama N, Sanada J. Imaging of benign hypervascular hepatocellular nodules in alcoholic liver cirrhosis: differentiation from hypervascular hepatocellular carcinoma. *J Comput Assist Tomogr* 2007: 557-563 [PMID: 17882031 DOI: 10.1097/RCT.0b013e3180305bfb]

10 **Whiting P**, Rutjes AW, Reitsma JB, Bossuyt PM, Kleijnen J. The

development of QUADAS: a tool for the quality assessment of studies of diagnostic accuracy included in systematic reviews. *BMC Med Res Methodol* 2003; **3**: 25 [PMID: 14606960 DOI: 10.1186/1471-2288-3-25]

11 **Zheng WW**, Zhou KR, Chen ZW, Shen JZ, Chen CZ, Zhang SJ. Characterization of focal hepatic lesions with SPIO-enhanced MRI. *World J Gastroenterol* 2002; **8**: 82-86 [PMID: 11833077]

12 **Harisinghani MG**, Saini S, Weissleder R, Halpern EF, SchimaW, RubinDL, StillmanAE, SicaGT, SmallWC, HahnPF. Differentiation of liver hemangiomas from metastases and hepatocellular carcinoma at MR imaging enhanced with blood-pool contrast agent code-7227. *Radiology* 1997; **202**: 687-691 [DOI: 10.1148/radiology.202.3.9051017]

13 **Liver Cancer Study Group of Japan**. Classification of primary liver cancer. Tokyo, Japan: Kanehara & Co, 1997

14 **International Working Party**. Terminology of nodular hepatocellular lesions. *Hepatology* 1995; **22**: 983-993 [PMID: 7657307 DOI: 10.1002/hep.1840220341]

15 **Lim JH**, Choi D, Cho SK, Kim SH, Lee WJ, Lim HK, Park CK, Paik SW, Kim YI. Conspicuity of hepatocellular nodular lesions in cirrhotic livers at ferumoxides-enhanced MR imaging: importance of Kupffer cell number. *Radiology* 2001; **220**: 669-676 [PMID: 11526265 DOI: 10.1148/radiol.2203001777]

16 **Yoon MA**, Kim SH, Park HS, Lee DH, Lee JY, Han JK, Choi BI. Value of dual contrast liver MRI at 3.0T in differentiating well-differentiated hepatocellular carcinomas from dysplastic nodules: preliminary results of multivariate analysis. *Invest Radiol* 2009; **44**: 641-649 [DOI: 10.1097/RLI.0b013e3181ab6e57]

17 **Paley MR**, Mergo PJ, Torres GM, Ros PR. Characterization of focal hepatic lesions with ferumoxides-enhanced T2-weighted MR imaging. *AJR Am J Roentgenol* 2000; **175**: 159-163 [PMID: 10882267 DOI: 10.2214/ajr.175.1.1750159]

18 **Park HS**, Lee JM, Kim SH, Chang S, Kim SJ, Han JK, Choi BI. Differentiation of well-differentiated hepatocellular carcinomas from other hepatocellular nodules in cirrhotic liver: value of SPIO-enhanced MR imaging at 3.0 Tesla. *J Magn Reson Imaging* 2009; **29**: 328-335 [PMID: 19161184 DOI: 10.1002/jmri.21615]

19 **Imai Y**, Murakami T, Yoshida S, Nishikawa M, Ohsawa M, Tokunaga K, Murata M, Shibata K, Zushi S, Kurokawa M, Yonezawa T, Kawata S, Takamura M, Nagano H, Sakon M, Monden M, Wakasa K, Nakamura H. Superparamagnetic iron oxide-enhanced magnetic resonance images of hepatocellular carcinoma: correlation with histological grading. *Hepatology* 2000; **32**: 205-212 [PMID: 10915725 DOI: 10.1053/jhep.2000.9113]

20 **Zhang XH**, Liang BL, Huang SQ. [Correlation between SPIO-enhanced magnetic resonance imaging (MRI) and histological grading in hepatocellular carcinoma]. *Ai Zheng* 2003; **22**: 734-738 [PMID: 12866966]

21 **Suzuki S**, Iijima H, Moriyasu F, Sasaki S, Yanagisawa K, Miyahara T, Oguma K, Yoshida M, Horibe T, Ito N, Kakizaki D, Abe K, Tsuchiya K. Differential diagnosis of hepatic nodules using delayed parenchymal phase imaging of levovist contrast ultrasound: comparative study with SPIO-MRI. *Hepatol Res* 2004; **29**: 122-126 [PMID: 15163434 DOI: 10.1016/j.hepres.2004.02.010]

22 **Kato H**, Kanematsu M, Kondo H, Goshima S, Matsuo M, Hoshi H, Moriyama N. Ferumoxide-enhanced MR imaging of hepatocellular carcinoma: correlation with histologic tumor grade and tumor vascularity. *J Magn Reson Imaging* 2004; **19**: 76-81 [PMID: 14696223 DOI: 10.1002/jmri.10425]

23 **Okada M**, Imai Y, Kim T, Kogita S, Takamura M, Kumano S, Onishi H, Hori M, Fukuda K, Hayashi N, Wakasa K, Sakamoto M, Murakami T. Comparison of enhancement patterns of histologically confirmed hepatocellular carcinoma between gadoxetate- and ferucarbotran-enhanced magnetic resonance imaging. *J Magn Reson Imaging* 2010; **32**: 903-913 [PMID: 20882621 DOI: 10.1002/jmri.22333]

24 **Inoue T**, Kudo M, Watai R, Pei Z, Kawasaki T, Minami Y, Chung H, Fukunaga T, Awai K, Maenishi O. Differential diagnosis of nodular lesions in cirrhotic liver by post-vascular phase contrast-enhanced US with Levovist: comparison with superparamagnetic iron oxide magnetic resonance images. *J Gastroenterol* 2005; **40**: 1139-1147 [PMID: 16378178 DOI: 10.1007/s00535-005-1712-y]

25 **Chou CT**, Chen RC, Chen WT, Lii JM. Characterization of hyperintense nodules on T1-weighted liver magnetic resonance imaging: comparison of Ferucarbotran-enhanced MRI with accumulation-phase FS-T1WI and gadolinium-enhanced MRI. *J Chin Med Assoc* 2011; **74**: 62-68 [PMID: 21354082 DOI: 10.1016/j.jcma.2011.01.013]

P- Reviewer: Tang Y, Zhang BB **S- Editor**: Qi Y
L- Editor: AmEditor **E- Editor**: Ma S

Published by **Baishideng Publishing Group Inc**
8226 Regency Drive, Pleasanton, CA 94588, USA
Telephone: +1-925-223-8242
Fax: +1-925-223-8243
E-mail: bpgoffice@wjgnet.com
Help Desk: http://www.wjgnet.com/esps/helpdesk.aspx
http://www.wjgnet.com

ISSN 1007-9327